# Shape from shading with variable albedo

**Ping-Sing Tsai**
**Mubarak Shah,** MEMBER SPIE
University of Central Florida
Department of Computer Science
Computer Vision Laboratory
Orlando, Florida 32816
E-mail: shah@sono.cs.ucf.edu

**Abstract.** Most traditional shape-from-shading algorithms assume that an image contains only a single object with Lambertian surface and uniform albedo values. These algorithms perform poorly on images with nonuniform albedo values. In this paper, we first discuss a linear shape-from-shading method that employs discrete approximations for the surface normal using finite differences of the depth and linearizes the reflectance function in depth directly. Next we present a simple method to cancel the effect of albedo variation. In our approach, we first estimate the albedo values for each pixel, and segment the scene into regions with uniform albedo values. However, the estimated albedo values are not accurate at the points near edges, so we apply a modified median filter to improve the result. Then we adjust the intensity value for each pixel by dividing by the corresponding albedo value before applying the linear shape-from-shading method. Experimental results are presented for several synthetic and actual images.  [S0091-3286(97)03710-0]

Subject terms: physics-based vision; shape-from-shading; albedo estimate.

Paper 33027 received Feb. 24, 1997; accepted for publication June 7, 1997.

## 1 Introduction

Shape from shading (SFS) is one of the classic problems in computer vision, which deals with the recovery of 3-D shape from a *single* monocular image. The recovered shape can be expressed in terms of the depth $Z$, the surface normal $(n_x,n_y,n_z)$, the surface gradient $(p,q)$, or the surface slant $\phi$ and tilt $\theta$. This problem was formally introduced by Horn[1] in the early 1970s. Since then it has received considerable attention, and several efforts have been made to improve the shape recovery. Recently, Zhang et al.[2] implemented several well-known SFS methods[3–8] and presented a performance evaluation for them.

In SFS, the imaging model for expressing the relationship between surface shape and image brightness is specified through a proper reflectance map. Most traditional SFS algorithms use three assumptions: a single object with Lambertian surface and uniform albedo, a point light source, and orthographic projection. The reflectance equation can be written as

$$I=R(p,q)=\rho(\mathbf{N}\cdot\mathbf{L}), \tag{1}$$

where $I$ is the image brightness, $R$ is the reflectance function with $p$ and $q$ giving the surface gradient, $\rho$ is the composite albedo, $\mathbf{N}$ is the surface normal, and $\mathbf{L}$ is the light-source direction.

These assumptions are simple but restrictive. In the real world, there are many images that violate them. For example, none of the existing SFS methods can correctly recover the shape of a soccer ball, because the surface of a soccer ball does not have uniform albedo (there are black and white patches on the surface). In this paper, we present an approach to deal with images containing variable albedo values. We first estimate the albedo value for each pixel in an image using Lee and Rosenfeld's local albedo estimation method,[9] and then segment the scene into regions with uniform albedo values. However, due to the inaccuracy in the albedo estimate, there are some small regions near edges that have incorrect albedo values. Therefore, we apply a modified median filter to improve the result of segmentation. Then we adjust the intensity value for each pixel by dividing by the corresponding albedo value before applying the linear shape-from-shaping method.

This paper is organized as follows. In Sec. 2 we review several SFS and albedo estimation methods. A linear SFS method is presented in Sec. 3. Section 4 deals with images with variable albedo values. We explain how we can use Lee and Rosenfeld's local albedo estimation method[9] to cancel the effect of albedo variation before applying any SFS algorithm. Experimental results are presented in Sec. 5.

## 2 Review of Related Work

In this section, we briefly review SFS and albedo estimation methods.

### 2.1 *SFS Methods*

Several SFS methods are based on variational formulations, in which the surface normals (or surface gradient and depth) are determined by minimizing an energy function over the entire image. Zheng and Chellappa[4] considered the intensity-gradient constraint in the variational approach. Their energy function contains the brightness constraint [which is derived directly from the image irradiance equation (1)], the intensity-gradient constraint (which requires that the intensity gradient of the reconstructed image be close to the intensity gradient of the input image), and the integrability constraint (which ensures valid surfaces). The Euler equations were simplified by taking the Taylor series of the reflectance map and representing the depth, the gra-

 0091-3286/98/$10.00 

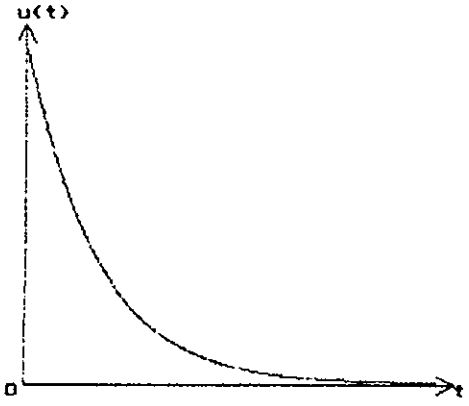


**Fig. 5** Result of step input.

tesimal disturbance, the nonlinear phase mutual coupling can be approximately regraded as linear. Therefore, each channel also can be approximately regarded as a multi-input-single-output linear controlling system, and each is independent. By the preceding approximation we can simplify the research on the dynamics of a multidither adaptive optical system to that of a linear controlling system, thus we can use the relative theory on linear controlling systems to analyze and research the dynamics of an adaptive optical system.

Under the condition of disturbance, the standards of system's optimum are (1) the stabilizing time is shortest, (2) the final light intensity is greatest, and (3) the stability of system is best.

## References

1. Y. Jiaxiong and Y. Yonglin, *Adaptive Optics*, Huazhong University of Science and Technology Press, Wuhan, China (Oct. 1992).
2. L. Shishi and L. Shida, *Special Function*, Meteorological Press, Beijing, China (May 1988).
3. X. Linge, *Automatic Controlling Principle*, Electric Power Industrial Press, Beijing, China (June 1986).
4. D. Bixin, *Fundament of Signal Analysis*, Beijing University of Science & Technology Press, Beijing, China (June 1994).
5. L. Qinyang, W. Nengchao, and Y. Dayi, *Numerical Analysis*, Huazhong University of Science & Technology Press, Wuhan, China (July 1995).

**Youbin Fang** is a master candidate in the Department of Photoelectric Engineering at Huazhong University of Science & Technology and will graduate in June 1998. His current research interests include adaptive optics and optical and fiber communication.

**Xueming Zhang** graduated from the Institute of Modern Optics at Naikai University and received his MS degree in 1994. He has been a lecturer in the Department of Photoelectric Engineering at Huazhong University of Science & Technology since then, where his current research interests include fiber optics, optical communication, and nonlinear optics.

**Jiaxiong Ye** is a professor in the Department of Photoelectric Engineering at Huazhong University of Science & Technology. He graduated from the Automatic Control Department of Tsinghua University and received his BS degree in 1960. His current research interests include optical communication, nonlinear optics, adaptive optics, optical disks, and binary optics.

dient, and their derivatives in discrete form. Then, an iterative scheme, which updates depth and gradient simultaneously, was derived. The algorithm was implemented using a hierarchical structure (pyramid) in order to speed up the computation. The initial values for both depth and gradient can be zero.

Lee and Kuo's approach[5] involves the brightness constraint and the smoothness constraint. Surfaces were approximated by the union of triangular surface patches. The vertices of the triangles were called nodal points, and only nodal depths were recovered. Depths at the pixels that are not nodal points were obtained through interpolation. For each triangular patch, the intensity of the triangle was taken as the average intensity of all pixels in the triangle, and the surface gradient of the triangle was approximated by the cross product of any two adjacent edges of the triangle. This established a relationship between the triangle's intensity and the depth at its three nodal points. Linearizing the reflectance map in terms of the surface gradient $(p,q)$, a linear relationship between the intensity and depth at the nodal points was derived. The surface depths at the nodal points were computed using optimization. The optimization problem was reduced to the solution of a sparse linear system, and a multigrid computational algorithm was applied to solve for the depth.

Following the main idea of Dupuis and Oliensis[10,11] (singular-point constraints), Bichsel and Pentland[6] developed an efficient minimum downhill approach that recovers depth and guarantees a continuous surface. Given initial values at the singular points (brightest points), the algorithm looks in eight discrete directions in the image and propagates the depth information away from the light source to ensure the proper termination of the process. Since the slopes at the surface points in low-brightness regions are close to zero for most directions (except the directions that make a very narrow angle with the illumination direction), the image was initially rotated to align the light-source direction with one of the eight directions. The inverse rotation was performed on the resulting depth map in order to get the original orientation back.

Pentland[8] used the linear approximation of the reflectance function in terms of the surface gradient, and applied a Fourier transform to the linear function to get a closed-form solution for the depth at each point. This yields a noniterative algorithm.

### 2.2 *Albedo Estimation Methods*

Two statistical approaches for estimating albedo were reported by Lee and Rosenfeld[7] and Zheng and Chellappa.[4] The major difference between these two methods lies in their assumptions about the distribution of surface normals. Lee and Rosenfeld[7] assumed the surface patches to be locally spherical and used a Gaussian sphere to derive the probability density function of the surface-normal tilt $(\tau)$ and slant $(\sigma)$, $f_{\tau\sigma}$, as $f_{\tau\sigma}=(1/2\pi)\sin 2\sigma$. Zheng and Chellappa[4] assumed the surface patches to be locally flat, and $\tau$ and $\sigma$ to be independent of each other. They used $f_\tau = 1/2\pi$ as the distribution of tilt, and assumed that slant is uniformly distributed in 3-D space. Therefore, the statistical model for the distribution of surface normals is $f_{\tau\sigma} = f_\tau f_\sigma = (1/2\pi)\cos\sigma$. However, both of them assumed uniform albedo for the whole image.

Lee and Rosenfeld[9] presented another albedo estimation method for scene segmentation. They computed the composite albedo value $\rho$ for each pixel, using only the local intensity information. Let $I_P$ denotes the image intensity at point $P$, let $Q$ be a point near $P$ in the gradient direction at $P$, and let $R$ be a point on the opposite side of $P$. Let

$$I_P=\rho(\mathbf{N}_P\cdot\mathbf{l})=\rho\cos\theta, \tag{2}$$

$$I_Q=\rho(\mathbf{N}_Q\cdot\mathbf{l})=\rho\cos(\theta+\delta\theta_1), \tag{3}$$

$$I_R=\rho(\mathbf{N}_R\cdot\mathbf{l})=\rho\cos(\theta-\delta\theta_2), \tag{4}$$

where $\mathbf{N}_P$, $\mathbf{N}_Q$, and $\mathbf{N}_R$ are the surface normals respectively at $P$, $Q$, and $R$; $\theta$ is the angle between $\mathbf{N}_P$ and the light-source direction $\mathbf{l}$; and $\delta\theta_1$, $\delta\theta_2$ are positive and small. They approximated $\delta\theta_1\approx\delta\theta_2=\delta\theta$. The system (2)–(4) consists of three equations with three unknowns $\rho$, $\theta$, and $\delta\theta$. After some algebraic manipulation, the albedo value for $P$ is given by

$$\rho^2=\frac{I_P^2-I_RI_Q}{I_P^2-[(I_R+I_Q)/2]^2}\,I_P^2. \tag{5}$$

(Note that if $P$, $Q$, and $R$ lie in a plane, this method breaks down because the denominator becomes zero.)

## 3 Linear Shape-from-Shading Method

We have proposed a linear shape-from-shading method.[11] In this method, we first apply the discrete approximation of the gradient $(p,q)$, and then directly employ the linear approximation of the reflectance function in terms of the depth $Z$. The reflectance function for Lambertian surfaces is modeled as follows:

$$I_{i,j}=R(p,q) \tag{6}$$

$$=\frac{1+pp_s+qq_s}{(1+p^2+q^2)^{1/2}(1+p_s^2+q_s^2)^{1/2}}$$

$$=\frac{\cos\sigma+p\cos\tau\sin\sigma+q\sin\tau\sin\sigma}{(1+p^2+q^2)^{1/2}}, \tag{7}$$

where $I_{i,j}$ is the gray level at pixel $(i,j)$, $p=\partial Z_{i,j}/\partial x$, $q=\partial Z_{i,j}/\partial y$, $p_s=(\cos\tau\sin\sigma)/\cos\sigma$, $q_s=(\sin\tau\sin\sigma)/\cos\sigma$, $\tau$ is the tilt of the illuminant, and $\sigma$ is the slant of the illuminant. Using finite-difference discrete approximations $p=Z_{i,j}-Z_{i-1,j}$ and $q=Z_{i,j}-Z_{i,j-1}$ for $p$ and $q$, the reflectance equation can be rewritten as

$$0=f(I_{i,j},Z_{i,j},Z_{i-1,j},Z_{i,j-1})=I_{i,j}-R(Z_{i,j}-Z_{i-1,j},Z_{i,j}-Z_{i,j-1}). \tag{8}$$

For a fixed point $(i,j)$ and a given image $I$, a linear approximation (Taylor series expansion up through the first-order terms) of the function $f$ [Eq. (8)] about a given depth map $Z^{n-1}$ is

$$
\begin{aligned}
0 &= f(I_{i,j}, Z_{i,j}, Z_{i-1,j}, Z_{i,j-1}) \\
&\approx f(I_{i,j}, Z_{i,j}^{n-1}, Z_{i-1,j}^{n-1}, Z_{i,j-1}^{n-1}) + (Z_{i,j} - Z_{i,j}^{n-1}) \\
&\quad \times \frac{\partial}{\partial Z_{i,j}} f(I_{i,j}, Z_{i,j}^{n-1}, Z_{i-1,j}^{n-1}, Z_{i,j-1}^{n-1}) + (Z_{i-1,j} - Z_{i-1,j}^{n-1}) \\
&\quad \times \frac{\partial}{\partial Z_{i-1,j}} f(I_{i,j}, Z_{i,j}^{n-1}, Z_{i-1,j}^{n-1}, Z_{i,j-1}^{n-1}) + (Z_{i,j-1} - Z_{i,j-1}^{n-1}) \\
&\quad \times \frac{\partial}{\partial Z_{i,j-1}} f(I_{i,j}, Z_{i,j}^{n-1}, Z_{i-1,j}^{n-1}, Z_{i,j-1}^{n-1}). \qquad (9)
\end{aligned}
$$

The above equation can be written as follows:

$$
\begin{aligned}
&\frac{\partial}{\partial Z_{i,j-1}} f(I_{i,j}, Z_{i,j}^{n-1}, Z_{i-1,j}^{n-1}, Z_{i,j-1}^{n-1}) Z_{i,j-1} \\
&\quad + \frac{\partial}{\partial Z_{i-1,j}} f(I_{i,j}, Z_{i,j}^{n-1}, Z_{i-1,j}^{n-1}, Z_{i,j-1}^{n-1}) Z_{i-1,j} \\
&\quad + \frac{\partial}{\partial Z_{i,j}} f(I_{i,j}, Z_{i,j}^{n-1}, Z_{i-1,j}^{n-1}, Z_{i,j-1}^{n-1}) Z_{i,j} \\
&\quad = -f(I_{i,j}, Z_{i,j}^{n-1}, Z_{i-1,j}^{n-1}, Z_{i,j-1}^{n-1}) \\
&\qquad + Z_{i,j}^{n-1} \frac{\partial}{\partial Zi,j} f(I_{i,j}, Z_{i,j}^{n-1}, Z_{i-1,j}^{n-1}, Z_{i,j-1}^{n-1}) \\
&\qquad + Z_{i-1,j}^{n-1} \frac{\partial}{\partial Z_{i-1,j}} f(I_{i,j}, Z_{i,j}^{n-1}, Z_{i-1,j}^{n-1}, Z_{i,j-1}^{n-1}) \\
&\qquad + Z_{i,j-1}^{n-1} \frac{\partial}{\partial Z_{i,j-1}} f(I_{i,j}, Z_{i,j}^{n-1}, Z_{i-1,j}^{n-1}, Z_{i,j-1}^{n-1}),
\end{aligned}
$$

or in vector form as follows:

$$
(0,\ldots, a_{i,j-1}, 0,\ldots, a_{i-1,j}, a_{i,j}, 0\ldots) \begin{pmatrix} Z_{1,1} \\ \vdots \\ Z_{i,j} \\ \vdots \\ Z_{M,M} \end{pmatrix} = b_{i,j}, \qquad (10)
$$

where $a_{i,j} = (\partial / \partial Z_{i,j}) f(I_{i,j}, Z_{i,j}^{n-1}, Z_{i-1,j}^{n-1}, Z_{i,j-1}^{n-1})$ and

$$
\begin{aligned}
b_{i,j} &= -f(I_{i,j}, Z_{i,j}^{n-1}, Z_{i-1,j}^{n-1}, Z_{i,j-1}^{n-1}) \\
&\quad + Z_{i,j}^{n-1} \frac{\partial}{\partial Z_{i,j}} f(I_{i,j}, Z_{i,j}^{n-1}, Z_{i-1,j}^{n-1}, Z_{i,j-1}^{n-1}) \\
&\quad + Z_{i-1,j}^{n-1} \frac{\partial}{\partial Zi-1,j} f(I_{i,j}, Z_{i,j}^{n-1}, Z_{i-1,j}^{n-1}, Z_{i,j-1}^{n-1}) \\
&\quad + Z_{i,j-1}^{n-1} \frac{\partial}{\partial Z_{i,j-1}} f(I_{i,j}, Z_{i,j}^{n-1}, Z_{i-1,j}^{n-1}, Z_{i,j-1}^{n-1}).
\end{aligned}
$$

For an $M$-by-$M$ image, there are $M^2$ such equations, which will form a linear system $AZ = B$, where $A$ is an $M^2 \times M^2$ matrix, and $Z$ and $B$ are $M^2 \times 1$ vectors. This linear system is difficult to solve directly, since it will involve the inversion of a huge matrix, $A$. However, it can be solved easily using the Jacobi iterative method.

Now, let us look carefully inside the Jacobi iterative method. For a given initial approximation $Z^0$, each depth value is solved for sequentially in an iteration. For example, the depth value $Z_{i,j}$ at the $n$'th iteration can be solved for using the previous estimates, $Z_{i',j'}^{n-1}$, for all the $Z_{i',j'}$ with $i' \neq i$ and $j' \neq j$. When $Z_{i-1,j}^{n-1}$ and $Z_{i,j-1}^{n-1}$ are respectively substituted for $Z_{i-1,j}$ and $Z_{i,j-1}$ in Eq. (9), the third and fourth terms on the right-hand side vanish. Therefore, Eq. (9) reduces to the surprisingly simple form given in the following equation:

$$
0 = f(Z_{i,j}) \approx f(Z_{i,j}^{n-1}) + (Z_{i,j} - Z_{i,j}^{n-1}) \frac{\mathrm{d}}{\mathrm{d}Z_{i,j}} f(Z_{i,j}^{n-1}). \qquad (11)
$$

Then for $Z_{i,j} = Z_{i,j}^{n}$, the depth map at the $n$'th iteration, can be found directly as follows:

$$
Z_{i,j}^{n} = Z_{i,j}^{n-1} + \frac{-f(Z_{i,j}^{n-1})}{(\mathrm{d}/\mathrm{d}Z_{i,j}) f(Z_{i,j}^{n-1})}, \qquad (12)
$$

where

$$
\begin{aligned}
\frac{\mathrm{d}f(Z_{i,j}^{n-1})}{\mathrm{d}Z_{i,j}} = -1 \times \Bigg[ & \frac{p_s + q_s}{(p^2+q^2+1)^{1/2}(p_s^2+q_s^2+1)^{1/2}} \\
& - \frac{(p+q)(pp_s+qq_s+1)}{(p^2+q^2+1)^{3/2}(p_s^2+q_s^2+1)^{1/2}} \Bigg].
\end{aligned}
$$

Now, assuming the initial estimate of $Z^0(x,y) = 0$ for all pixels, the depth map can be refined iteratively using Eq. (12). This method is simple and efficient, and yields better results for images with central illumination or low-angle illumination.

## 4 SFS for Images with Variable Albedo Values

The linear SFS method described in the previous section, like the majority of other SFS methods, assumes that objects in the scene have uniform albedo. Consequently, they cannot be applied directly to images containing surfaces with nonuniform albedo. For example, when we apply the linear method (as described in the previous section) to the image of a flower with three albedo values [as shown in Fig. 5(a) of Sec. 5], we obtain a depth map [as shown in Fig. 1(a)] with different height between the petals and the central region of the flower, which is incorrect. This is simply due to the albedo variation. Similarly, when we apply Pentland's method,[8] Bichsel and Pentland's method,[6] and Zheng and Chellappa's method[4] to the same image, we obtain wrong depth estimations as shown in Fig. 1(b) to 1(d). Lee and Kuo's method[5] does not even converge on this image.

In order to get the correct result, we need to cancel the effect of albedo variation before applying any SFS algorithm. To cancel the effect of albedo variation, we need to compute the albedo value for each pixel. The two statistical approaches are no longer applicable here, because they attempt to estimate a constant albedo value for all pixels in the scene. The local-estimate method, which assumes only that neighboring points have the same albedo values, is

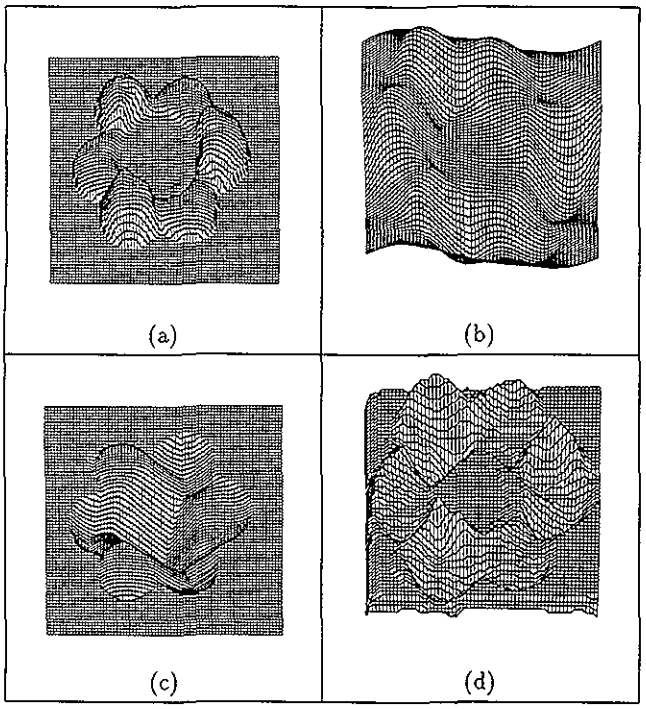


**Fig. 1** Results for SFS methods: (a) the linear SFS method, (b) Pentland's method, (c) Bichsel and Pentland's method, (d) Zheng and Chellapa's method.

more appropriate for our purpose. However, the estimated albedo value for each pixel is not very accurate for real images, especially for the points near edges. Therefore, we will segment the scene first, according to the estimated albedo values, into different regions, and assign a single albedo value to each region. The segmentation is done using a simple histogram-based approach. We have noted that due to the inaccuracy in the albedo estimate, some small regions near the edges are misclassified. Therefore, these small regions have incorrect albedo values. Lee and Rosenfeld[9] used the median filter to avoid interactions across edges. However, the standard median filter can deal only with values specified over the whole scene, not over a small region. We apply a modified median filter, in which we replace the albedo value of each pixel by the median of the nonzero albedo values (pixels with zero albedo value correspond to the background) in a predefined neighborhood of that pixel. The segmentation can be improved by applying this median filter several times.

After we obtain the albedo map for the scene, we adjust the intensity value for each pixel by dividing by the corresponding albedo value. Since the intensity value at each point is just the composite albedo value multiplied by the dot product of the surface normal and the illumination direction ($I = \rho \mathbf{N} \cdot \mathbf{L}$), the effect of albedo variation will be canceled by the intensity adjustment. Afterward, we can apply any SFS method to the adjusted intensity image to get the correct depth map.

## 5 Experimental Results

Our first experiment used a synthetic image of spheres [as shown in Fig. 2(a)]. These two spheres have the same depth values. However, the sphere on the left in the image was generated with albedo value 200, and the sphere on the right was generated with albedo value 255. Figure 2(b) shows the result obtained by applying the linear SFS method to the image without any intensity adjustment. We can see that the estimated depth map is incorrect, since the two spheres should have the same height. Figure 2(c) shows the estimated albedo map (which was obtained with Lee and Rosenfeld's method), and Fig. 2(d) shows the histogram. Figure 2(e) shows the albedo map after applying the histogram-based segmentation, and Fig. 2(f) shows the albedo map after appyling the modified median filter twice. Figure 2(g) shows the correct depth estimate (two spheres with the same height) that was obtained from the linear SFS method after the intensity adjustment using the estimated albedo map [Fig. 2(f)].

Figure 3 shows a real image containing a foam ball with two different albedo values. The image was taken with a standard camcorder and digitized on a Sun workstation. The light source direction is approximately (0,0,1), and the input image is shown in Fig. 3(a). The depth map computed by the linear SFS method is shown in Fig. 3(b). Figure 3(c) shows the estimated albedo map, and Fig. 3(d) shows the histogram. Figure 3(e) shows the albedo map after applying the histogram-based segmentation, and Fig. 3(f) shows the albedo map after applying the modified median filter. The depth map computed by the linear SFS method after intensity adjustment using the estimated albedo [Fig. 3(f)] is shown in Fig. 3(g). We can see that the correct depth values can be obtained easily after the intensity adjustment.

The results for a natural image containing a flower with two albedo values is shown in Fig. 4. The albedo value for the petals is higher than for the central region of the flower, and the central region of the flower should have approximately the same height as the petal region. The image was taken by a Sony CCD camera with a single fiber optic illuminator, and digitized on a Sun workstation. The input image is shown in Fig. 4(a), and the light-source direction is approximately (0,0,1). The linear SFS method produced an estimate with a large hole at the center [as shown in Fig. 4(b)]. This is due to the fact that the albedo of the central region is lower than the albedo of the petals. Figure 4(c) shows the estimated albedo map, and the histogram is shown in Fig. 4(d). Figure 4(e) shows the albedo map after applying the histogram-based segmentation, and Fig. 4(f) shows the albedo map after applying the modified median filter. A better depth estimate [as shown in Fig. 4(g)] was obtained by the proposed method.

Figure 5 shows the results for a real image of a three-albedo flower. The petals of the flower have two different albedo values, and the central region has the lowest albedo value. All the petals and the central region of the flower should have approximately the same height. The linear SFS method produced a depth map [as shown in Fig. 5(b)] with different heights for those regions. Figures 5(c) and 5(d) show the estimated albedo map and the histogram. Figure 5(e) shows the albedo map after applying the histogram-based segmentation, and Fig. 5(f) shows the albedo map after applying the modified median filter. The depth map

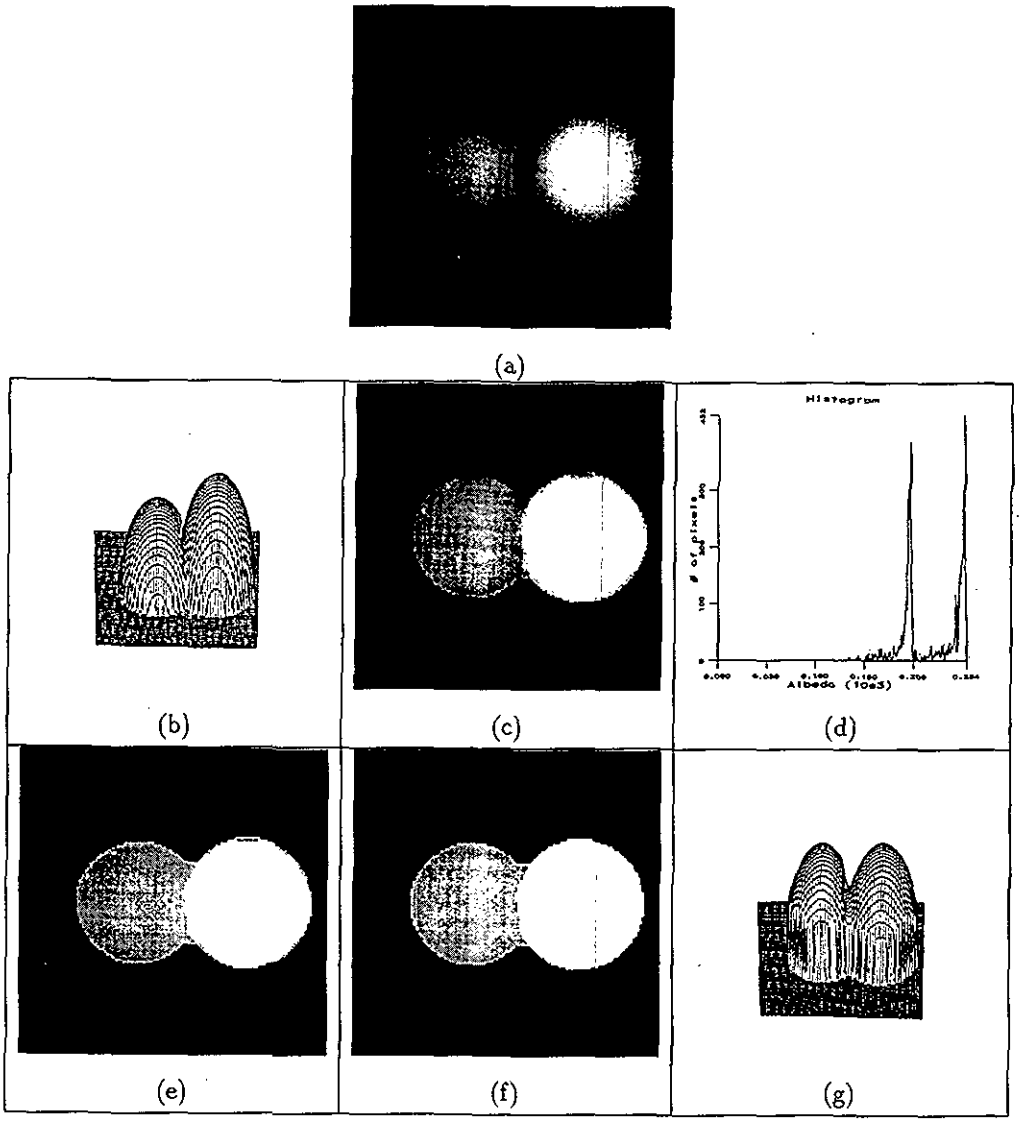


**Fig. 2** Results for a synthetic image of two spheres with different albedo values: (a) input image, (b) results obtained from the linear SFS method, (c) estimated albedo map using Lee and Rosefeld's method, (d) histogram for the estimated albedo map, (e) albedo map after histogram-based segmentation, (f) albedo map after applying the modified median filter twice, (g) results obtained from linear SFS method after intensity adjustment.

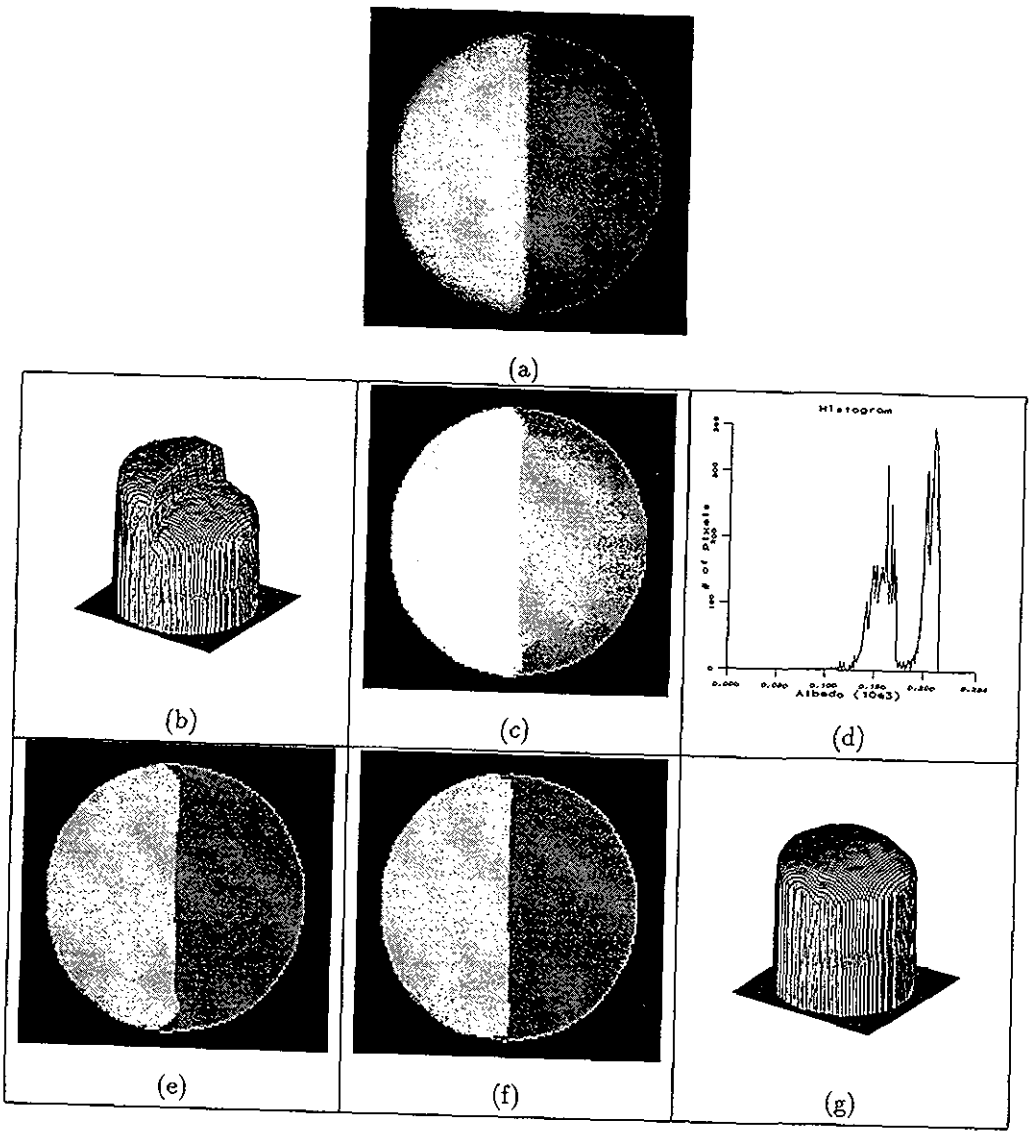


**Fig. 3** *Results for real image of a foam ball with two different albedo values: (a) input image, (b) results obtained from the linear SFS method, (c) estimated albedo map using Lee and Rosenfeld's method, (d) histogram for the estimated albedo map, (e) albedo map after histogram-based segmentation, (f) albedo map after applying the modified median filter, (g) results obtained from the linear SFS method after intensity adjustment.*

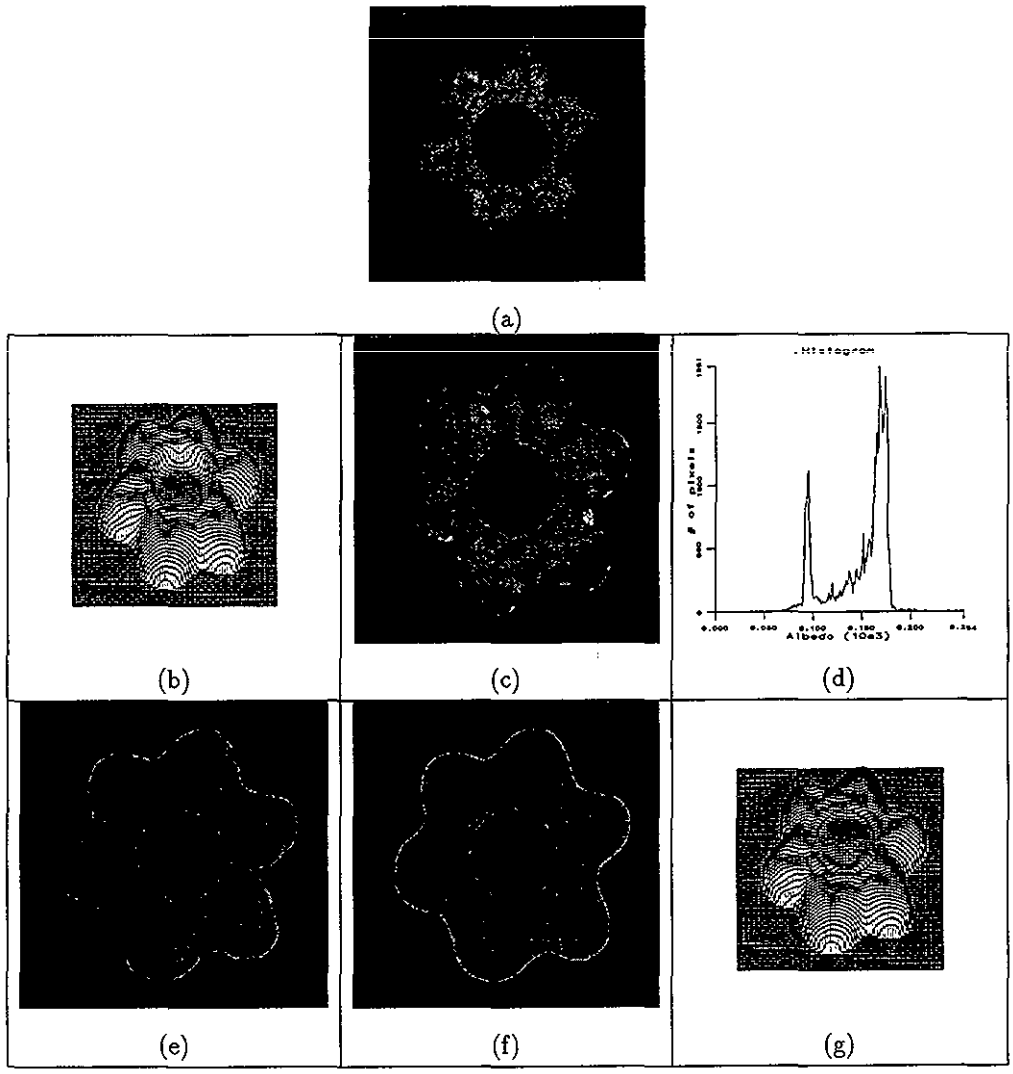


**Fig. 4** Results for an actual image of a flower with two different albedo values: (a) input image, (b) results obtained from the linear method, (c) estimated albedo map using Lee and Rosenfeld's method, (d) histogram for the estimated albedo map, (e) albedo map after histogram-based segmentation, (f) albedo map after applying the modified median filter, (g) results obtained from the linear method after intensity adjustment.

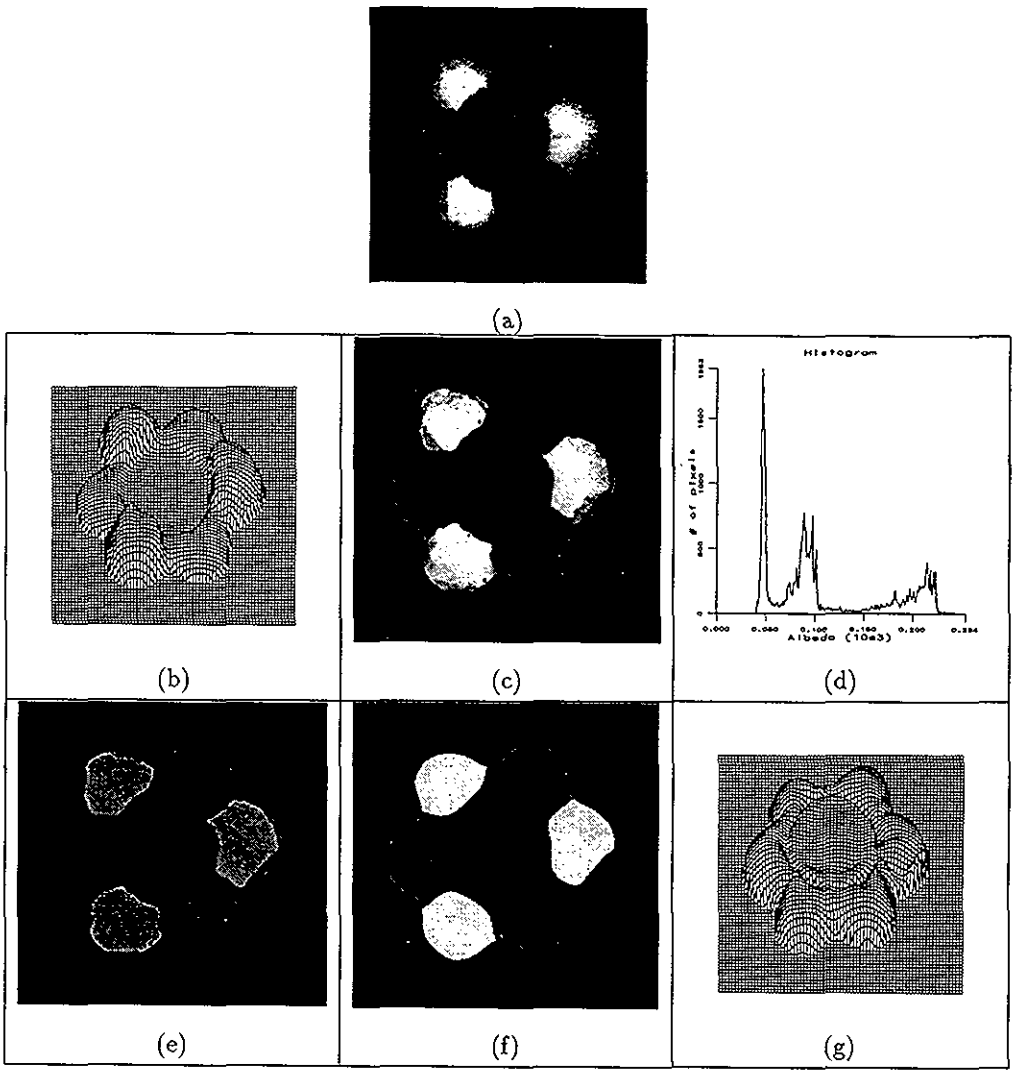


**Fig. 5** Results for an actual image of a flower with three different albedo values: (a) input image, (b) results obtained from the linear SFS method, (c) estimated albedo map using Lee and Rosenfeld's method, (d) histogram for the estimated albedo map, (e) albedo map after histogram-based segmentation, (f) albedo map after applying the modified median filter, (g) results obtained from the linear SFS method after intensity adjustment.

produced by the proposed method [as shown in Fig. 5(g)] is much better than the one without intensity adjustment.

## 6 Conclusions

Shape recovery from a single shaded image is a very important problem in computer vision. We have presented a linear SFS method and a simple way to cancel the effect of albedo variation before applying the SFS algorithm. The results of several synthetic and real images were presented to demonstrate our approach.

### References

1. B. K. P. Horn, Shape from shading: a method for obtaining the shape of a smooth opaque object from one view, PhD Thesis, MIT, 1970.
2. R. Zhang, P. S. Tsai, J. E. Cryer, and M. Shah, Analysis of shape from shading techniques, in *Proc. IEEE Computer Vision and Pattern Recognition*, pp. 377–384 (1994).
3. M. J. Brooks and B. K. P. Horn, Shape and source from shading, in *Proc. International Joint Conference on Artificial Intelligence*, pp. 932–936 (1985).
4. Q. Zheng and R. Chellappa, Estimation of illuminant direction, albedo, and shape from shading, *IEEE Trans. Pattern Anal. and Machine Intell.* **13**(7), 680–702 (1991).
5. K. M. Lee and C. C. J. Kuo, Shape from shading with a linear triangular element surface model, *IEEE Trans. Pattern Anal. and Machine Intell.* **15**(8), 815–822 (1993).
6. M. Bichsel and A. Pentland, A simple algorithm for shape from shading, in *Proc. IEEE Computer Vision and Pattern Recognition*, pp. 459–464 (1992).
7. C. H. Lee and A. Rosenfeld, Improved methods of estimating shape from shading using the light source coordinate system, *Artif. Intell.* **26** 125–143 (1985).
8. A. Pentland, Shape information from shading: a theory about human perception, in *Proc. IEEE Second International Conf. on Computer Vision*, pp. 404–413 (1988).
9. C. H. Lee and A. Rosenfeld, Albedo estimation for scene segmentation, *Pattern Recognition Lett.* **1**, 155–160 (1983).
10. P. Dupuis and J. Oliensis, Direct method for reconstructing shape from shading, in *Proc. IEEE Computer Vision and Pattern Recognition*, pp. 453–458 (1992).
11. J. Oliensis and P. Dupuis, A global algorithm for shape from shading, in *Proc. IEEE International Conf. on Computer Vision*, pp. 692–701 (1993).
12. P. S. Tsai and M. Shah, Shape from shading using linear approximation, *Image and Vision Comput.* **12**(8), 487–498 (1994).

**Ping-Sing Tsai** received the BS degree in information and computer engineering from Chung-Yuan Christian University in 1985, and his PhD in computer science at the University of Central Florida in 1995. Dr. Tsai is currently working at Intel Corporation, Digital Peripherals Division, as a senior system engineer.

**Mubarak Shah** received his BE degree in 1979 in electronics from Dawood College of Engineering and Technology, Karachi, Pakistan, and was awarded a five year Quad-e-Azam (Father of Nation) scholarship for his PhD. He spent 1980 at Philips International Institute of Technology, Eindhoven, The Netherlands, where he completed his EDE diploma. Dr. Shah received his MS and PhD degrees in computer engineering from Wayne State University, Detroit, Michigan, in 1982 and 1986, respectively. Since 1986 he has been with the University of Central Florida, where he is currently a professor of computer science and the director of the Computer Vision Lab. He was responsible for initiating the computer vision research and teaching area in his department. He received the TOKTEN award from UNDP in 1995, the Teaching Incentive Program award in 1995, and the IEEE Outstanding Engineering Educator award in 1997. Dr. Shah has served as a project director for the national site for Research Experience for Undergraduates (REU) in computer vision. He has co-edited one book, and has published more than 50 research papers in refereed journals on topics including visual motion, gesture recognition, lipreading, edge and contour detection, multisensor fusion, shape from shading and stereo, and hardware algorithms for computer vision. He is also interested in image compression, biomedical image analysis, visual databases, and digital libraries. He is an associate editor of *Pattern Recognition* and has served on the program committees and chaired sessions for several major conferences in computer vision. He was the organizer of a workshop on computer vision held in Islamabad, Pakistan, in January 1995.